LPNHE-94-01
Fermilab Library
0 1160 0039694 7

LPNHE 94-01
1993/07/22

MEASUREMENT OF THE PROTON STRUCTURE FUNCTION $F_2(x, Q^2)$ AT HERA

F(2)^(x,Q**2)

E

To Appear in the Proceedings of the International Europhysics Conference on High Energy Physics, Marseille, 22-28 July 1993.

Gregorio Bernardi
for the
H1 Collaboration

Paris Univ. VII, LPNHE

CN

Laboratoire de Physique Nucléaire
et de Hautes Energies

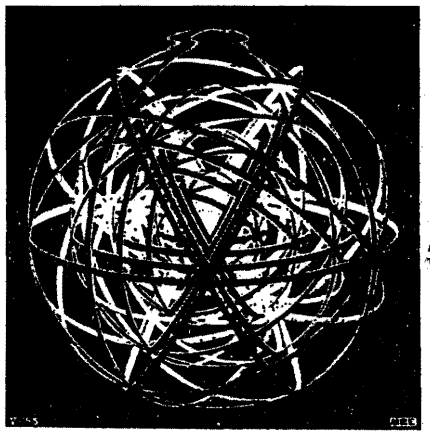

FERMILAB
MAY 09 1994

LPNHE - Paris

CNRS - IN2P3 - Universités Paris VI et VII
4, place Jussieu - Tour 33 - Rez-de-Chaussée
75252 Paris Cedex 05

Tél. : 33 (1) 44 27 63 13 - FAX. : 33 (1) 44 27 46 38 - Télex: 202 326 F

Measurement of the Proton Structure Function $F_2^p(x, Q^2)$ at HERA

Gregorio BERNARDI
*(**H1** collaboration)*
LPNHE, Université de Paris VI-VII
4 Place Jussieu, Paris 75005, France

ABSTRACT

We present the first results on the proton structure function $F_2(x, Q^2)$ at HERA, for $Q^2 > 5\ GeV^2$ and in the low Bjorken x range between 10^{-2} and 10^{-4}. The measurement is based on about 1100 neutral current deep inelastic scattering events recorded by the H1 detector in the first year of HERA operation, corresponding to an integrated luminosity of 22.5 nb^{-1}. At high Q^2 the measurement of the structure function $F_2(x, Q^2)$ is in good agreement within large statistical errors with QCD up to 720 GeV^2. At low Q^2, $F_2(x, Q^2)$ displays a significant rise when x is decreasing. A sizeable fraction ($\simeq 6\%$) of the events displays a large gap in rapidity between the remnant of the proton and the rest of the energy deposited by the hadronic final state.

Introduction

The commissionning in Spring 92 of HERA, the first *ep* collider ever built, allows to study deep inelastic scattering (d.i.s.) in a new kinematical domain. Very high momentum transfer collisions (Q^2 up to $5.10^4\ GeV^2$) can be studied, but also very low momentum fractions of the proton (x lower than 10^{-4}) can be reached at low Q^2. We expect in the low x region a deviation from the Altarelli-Parisi evolution equation since the terms in $\alpha_S \log \frac{1}{x}$ which appear in the higher order "ladder" diagrams [1] cannot be neglected anymore. The resummation of these terms is done in the Lipatov equation [2] which predicts a stronger rise of F_2^p in the low x region.

After a brief description of HERA, H1, the data reduction and the F_2 measurement methods, we will present our final results for the 92 data on F_2 in the low Q^2 region. We will then also give first conclusions from the high Q^2 sample and from a subsample of our low Q^2 d.i.s. sample which have a very peculiar final state: no energy is visible in the detector in the forward direction (defined as the incident proton direction), with a pseudo-rapidity $\eta > 1.8$.

HERA and the H1 detector

In 1992 HERA has collided 9 bunches of 820 GeV protons against 9 bunches of 26.7 GeV electrons. A 10th bunch (called pilot-bunch in the following) in both beams was circulating freely in order to study the beam-gas background which was found to be small for the structure function measurement. The integrated luminosity used in this analysis was measured to be 22.5 nb^{-1} via the reaction $e^-p \rightarrow e^-p\gamma$, in which the final e^- and the photon were simultaneously detected in specialized calorimeters (electron and photon "taggers") close to the beam pipe but at large distance from the main detector ($-30\ m$ and $-105\ m$, where the +z direction is given by the proton beam). A precise description of the detector can be found in [3]. Here we describe briefly only the main components used in this analysis.

The backward electromagnetic calorimeter (BEMC) is made of 88 lead/scintillator stacks with a $16 \times 16\ cm^2$ section and a depth of 22 radiation lengths, corresponding to about 1 interaction length. The covered angular range is $155^o < \theta_e < 174^o$ but we restrict the low Q^2 analysis to $160^o < \theta_e < 172.5^o$. A 1.5 cm space resolution on the reconstructed center of gravity of the deposited energy in a stack is achieved by making use of the 4 photodiodes which detect the wavelength shifted light from the scintillators. The absolute energy scale and the constant term of the BEMC resolution are determined using kinematical relations of the d.i.s. events: the energy of the scattered electron (E_e) can be expressed as a function of the angles of the hadronic system[1] (θ_h) and of the electron (θ_e) which are essentially independent of the BEMC energy measurement. From these studies we conclude that the energy scale of the BEMC is known to 2 % and its resolution is described by $\sigma(E_e)/E_e = 0.1/\sqrt{E_e} \oplus 0.42/E_e \oplus 0.03$, where E_e is in GeV. Charged hadrons deposit on average only a tiny fraction of their energy in the BEMC.

The BEMC is followed by an array of scintillators (TOF) which provide the timing information of crossing particles, allowing to veto upstream beam-wall interactions and accept events happening in the nominal interaction region. Before the BEMC is located the Backward proportional chamber (BPC) made of 4 wire planes and having an angular acceptance of $155.5^o - 174.5^o$. It provides a space point with a $\pm 3\ mm$ precision for charged particles entering in the BEMC which is used for low Q^2 events, both for particle identification and, in combination with the vertex position, for

[1] θ_h is defined by : $\tan \frac{\theta_h}{2} = \sum_{hadrons} E - p_z / \sum_{hadrons} p_T$.

θ_e determination.

Charged particle tracks are also measured in two concentric jet drift chamber modules (CJC) of angular acceptance $15^o - 165^o$. The resolution in p_T reached in 92 with a 1.15 Tesla field provided by a superconducting solenoidal coil was $\delta p_T/p_T^2 < 0.01$. The z-vertex position[2] is determined event by event, from at least one track reconstructed in the CJC. For low x d.i.s. events the resolution on the z-vertex measurement is $\pm 2\ cm$.

The energy of the hadronic system is measured in the highly segmented liquid argon calorimeter (LAr) [4], in the BEMC and in the instrumented iron backing calorimeter. The LAr calorimeter consists of an electromagnetic (e.m.) section with lead absorber and a hadronic section with stainless steel absorber. The e.m. part has a depth between 20 and 30 radiation lengths whereas the total depth of both calorimeters varies between 4.5 and 8 interaction lengths. The LAr calorimeter covers the angular range between 4° and 153°. The calibration of the LAr calorimeter stacks has been obtained from test beam measurements using electrons and pions between 3 and 210 GeV [5]. The e.m energy scale has been checked in the H1 detector to a 2% accuracy [6] by comparing the measured track momentum of electrons and positrons produced by cosmic muons with the corresponding energy deposition in the calorimetric cells. The absolute scale of the hadronic energy is presently known to 7% as determined from studies of the p_t balance for deep inelastic scattering events.

Data Reduction

Although there is no natural frontier between low and high Q^2, we divided our d.i.s. sample in these 2 categories depending if the scattered electron was in the BEMC or in the LAr calorimeter, since the experimental conditions are very different and the number of events is still too small to study exactly the transition region between the 2 calorimeters. Starting from 5.10^5 events collected in 1992, we ended with about a 1000 events in the low Q^2 sample ($5 < Q^2 < 80\ GeV^2$) and 80 in the high Q^2 one ($160 < Q^2 < 720\ GeV^2$). Here is a summary of the main reduction steps.

Low Q^2 sample

The events are triggered by a cluster of energy deposited in the BEMC above 4 GeV not vetoed by the TOF counters. The analysis being done on electrons above 10.4 GeV, the trigger efficiency is greater than 99%. The selection of the events is obtained by requesting that:
- the TOF counters display a correct timing for genuine ep collisions
- a charged track or a BPC hit is associated with a BEMC cluster of energy greater than 10.4 GeV
- a vertex is reconstructed within $\pm 50\ cm$ of the nominal interaction point (generally from the hadronic system).
- the quantity $\delta = \Sigma(E - p_z)$ of all particles, which by 4-momentum conservation must be equal to $2 \times E_e^{beam} = 53.4\ GeV$ is greater than 30 GeV. With this cut we get rid of an important fraction of photoproduction events in which the scattered electron is faked by a π^0 conversion or a $\gamma\pi^{\pm}$ overlap, while it escapes along the beam pipe thus not contributing to δ. In the same way, events in which a hard photon is radiated along the beam pipe are also greatly reduced, thus diminishing the importance of the necessary radiative corrections.

The electron identification, verified on simulated d.i.s. events, is done by asking a shower radius smaller than 5 cm and a track-cluster link. After this last step, we verified using the pilot bunch events that essentially no beam-related background is left in the d.i.s. sample The only significant remaining background is due to photoproduction and can be estimated from the subsample in which the scattered electron is detected in the electron tagger. It is lower than 30% in our lowest x, Q^2 bin which is the most affected one, and it becomes negligible for $y < 0.4$. This background is substracted statistically.

High Q^2 sample

The events were triggered either by a LAr trigger (typical threshold: 5 GeV), or by an independent track trigger, thus allowing cross-checks directly on our sample. For electrons above 15 GeV the trigger efficiency is $95 \pm 10\%$, while between 10 and 15 GeV it drops to $80 \pm 20\%$.

The selection is done after an off-line rejection of cosmics and halo muon events by requesting:
- one electromagnetic cluster with $p_T > 5\ GeV$ entirely contained in the LAr calorimeter and at least 2° away from the dead areas in ϕ of the detector.
- one reconstructed vertex within $\pm 50\ cm$ of the nominal interaction point
- a reconstructed $y_e < 0.7$ to get rid of beam gas and photoproduction background

The electron identification, verified on simulated d.i.s. events, is done by asking an isolation condition from the rest of the event, and by selecting the energy cluster of highest transverse momentum (p_T).

[2] the x-y position is known from the beam position with high accuracy ($< 1mm$).

F_2^p measurement

To estimate the differential cross-section $d^2\sigma/dxdQ^2$ we followed out two "independent" analysis methods:

Method I

The kinematics is obtained from the scattered electron, the hadrons being nevertheless needed to determine the vertex and to determine δ. The systematic errors and the reconstruction/selection efficiencies are estimated from the data in bins of $\sqrt{E_e}$ and θ_e well adapted to the properties of the detector and which allow to reach lower values of x. This method is very precise at low x but suffers at high x (low y) since $\frac{\delta y}{y} \simeq \frac{1}{y}\frac{\delta E}{E}$. It also implies larger radiative corrections.

Method II

Here we use Q^2 from the electron while y is reconstructed from the hadrons:

$$y_h = \frac{\sum_{hadrons} E - p_z}{2E_e^{beam}}$$

We then obtain x via : $x_{mix} = Q^2/ys$. This method is less sensitive to radiative corrections but needs a deeper understanding of the detector, in particular to the low hadronic energy response characterizing the low Q^2 events. To overcome this problem we make simultaneously use of charged tracks and of calorimetric cells which are not in a 15(25) cm radius tube along the extrapolation of the tracks in the e.m.(hadronic) calorimeter. This method is well suited for low y events, while it suffers at very low x since the hadronic system goes in the backward direction where the H1 hadronic instrumentation is weak.

These two methods are thus complementary. At high Q^2 we also cross-checked our results with a 3rd method where the kinematics is determined from θ_e and from θ_h.

Systematic Errors

In both methods we computed the differential cross-sections taking into account the detector smearing effects which in both binnings are always smaller than 10%, together with the efficiency and resolutions effects. The systematic errors were estimated by simulating the effects of uncertainty in the response of the detector: calibration of the BEMC (±2%), of the LAr (±2% for the e^-, ±7% for the hadrons), angular precision on the electron direction (±5 $mrad$), vertex reconstruction efficiency knowledge (±10%). Errors on the smearing acceptance corrections, on the bin center corrections and on the radiative corrections were also estimated. The total systematic error ranges between 15 and 26% in the different bin of x and Q^2, not including and overall luminosity/selection uncertainty of 8%.

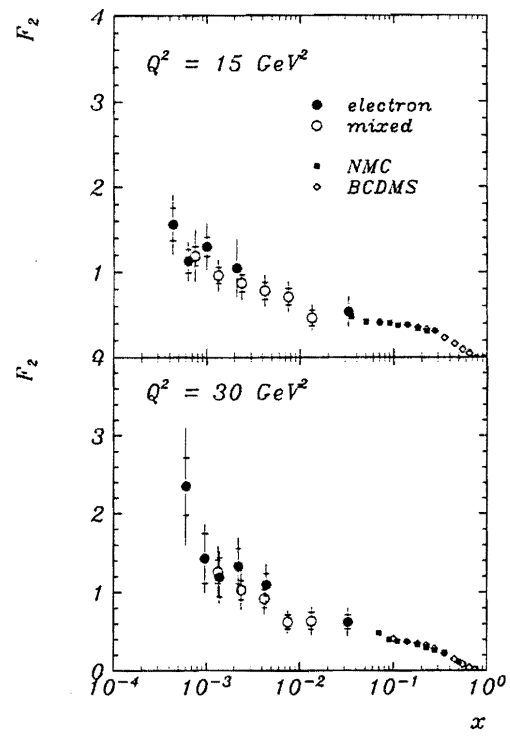

Figure 1: *F_2^p measurements of H1 with the 2 different methods compared with NMC and BCDMS results.*

The structure function F_2 is derived after radiative corrections (which have been estimated both numerically and analytically) via the following formula

$$\frac{d^2\sigma}{dxdQ^2} = \frac{2\pi\alpha^2}{xQ^4}(2 - 2y + \frac{y^2}{1+R})F_2(x, Q^2)$$

which is valid for $Q^2 << M_Z^2$ and where the parameter R which has not been measured yet at HERA has been taken according to the MRSD$^-$ structure function parametrization. As can be seen in fig.1, the observed agreement within errors of the 2 methods strengthens our results. Also visible is the good compatibility with previous experiments done at higher x[7, 8]. For the F_2^p measurement presented here after we chose for a given x, Q^2 bin the most precise method avoiding double counting of the events.

Results and Interpretation

The results are shown in fig.2 for different bins of

x and Q^2. A significant rise of F_2^p is visible at low x, in particular at low Q^2. The data favour the extrapolation at low x of the parametrization of previous F_2 measurements done including a sea quark and a gluon density $xG(x)$ diverging as $x^{-0.5}$ in the low x limit, like MRSD$^{-'}$ [9] reproduced in fig.2. The data clearly disfavour the extrapolation of other parametrizations like MRSD$^{0'}$ ($xG(x)$ constant at $Q^2 = 5\ GeV^2$) or CTEQ1MS [10] (slower sea quark density rise at low x). However before interpreting this rise as the effect predicted by the Lipatov equation we must notice that the simple GRV [11] extrapolation obtained by an Altarelli-Parisi evolution from a very low energy scale of valence-like partons is able to "predict" the effect we have observed. With the 93 data now available (20 times more integrated luminosity than in 92) we will hopefully settle the question, and reduce the large error bars on the high Q^2 points which are now consistent in the framework of QCD with the other points after Q^2 evolution.

Large rapidity gap events

A subsample of the d.i.s. events display somewhat surprizing properties already remarked by the ZEUS collaboration [12]: there is no visible energy flow in the forward calorimeter (e.g. for $\eta > 1.8$), so it exists a large rapidity gap between the proton remnants and the scattered parton. This is striking in fig.2a where the pseudo-rapidity of the most forward visible energy cluster (η_{max}) is plotted and compared to the Lepto montecarlo [13] which describes the other characteristics of the hadronic final state of our d.i.s. sample. In fact all the QCD inspired montecarlo programs which reproduce generally well the hadronic final state properties of our d.i.s. events [14] fail in producing such a subsample of events. A possible solution could be that the scattering does not occur on a parton of the proton, but on a pomeron-like colourless object emitted from the proton. In fig.2 b,c we display some properties of these events: the visible invariant mass is small and the number of charged central tracks has a peak at 2, hinting at possible diffractive vector meson production in d.i.s. In fig.2 d,e we plot the fraction of large rapidity gap events as a function of x and Q^2 and cannot observe any dependence on these variables with the present statistic thus showing that they do not account for the rise of F_2^p at low x. The effect of "diffractive" events with a smaller rapidity gap is still under study.

Conclusion

The first year of operation of HERA has allowed the first measurement of F_2^p at very low x by the 2 experiments H1 [6] and ZEUS [15]. Both experiments are in agreement and observe a rise of F_2^p with decreasing x. A subsample of peculiar d.i.s. events with a large rapidity gap between the "current jet" and the "remnant jet" has also been observed.

Acknowledgements

I am indebted to all my colleagues of the H1 deep inelastic analysis group for their joint effort in getting these results, in particular to J.F.Laporte for his help in preparing the figures.

References

[1] V.N.Gribov et al., *Phys. Rep.* **100** (1983) 1

[2] E.A.Kuraev,L.N.Lipatov and N.S.V.Fadin, *Phys. Lett.* **60B** (1975) 50; *Zh.E.T.F.* **72** (1977) 377

[3] H1 Collaboration, I. Abt et al., *The H1 Detector at HERA*, DESY preprint 93-103 (1993). See also A. DeRoeck, *these proceedings.*

[4] H1 Collaboration B. Andrieu et al., *The H1 Liquid Argon Calorimeter System*, DESY preprint 93-078 (1993). to be published in Nucl. Instr. and Meth.

[5] H1 Calorimeter Group, B. Andrieu et al., *Results from pion calibration runs for the H1 liquid argon calorimeter and comparisons with simulations*, DESY preprint 93-047 (1993), to be published in Nucl. Instr. and Meth.

[6] H1 Collaboration, I.Abt et al., *Nucl. Phys.* **B407** (1993) 515

[7] NMC Collaboration, P. Amaudruz et al., *Phys. Lett.* **295B** (1992) 159, and Erratum to CERN-PPE/92-124, CERN, April 1993.

[8] BCDMS Collaboration, A.C. Benvenuti et al.,*Phys.Lett.* **223B** (1989) 485.

[9] A.D.Martin et al., *Phys. Lett.*, **B306** (1993) 145, *ibid.*, **B309** (1993) 492

[10] J.Botts et al., *Phys. Lett.* **304B** (1993) 159

[11] M.Gluck et al., *Z Phys.* **C53** (1992) 127

[12] ZEUS Collaboration, M.Derrick et al., *Phys. Lett.* **B315** (1993) 481

[13] G. Ingelman, *"LEPTO 5.2", program manual*; H.Bengtsson, G.Ingelman, and T.Sjöstrand, *Nucl. Phys.***B301** (1988) 55

[14] H1 Collaboration, T. Ahmed et al., *Phys. Lett.* **298B** (1993) 469.

[15] ZEUS Collaboration, M.Derrick et al., DESY preprint 93-110 (1993)

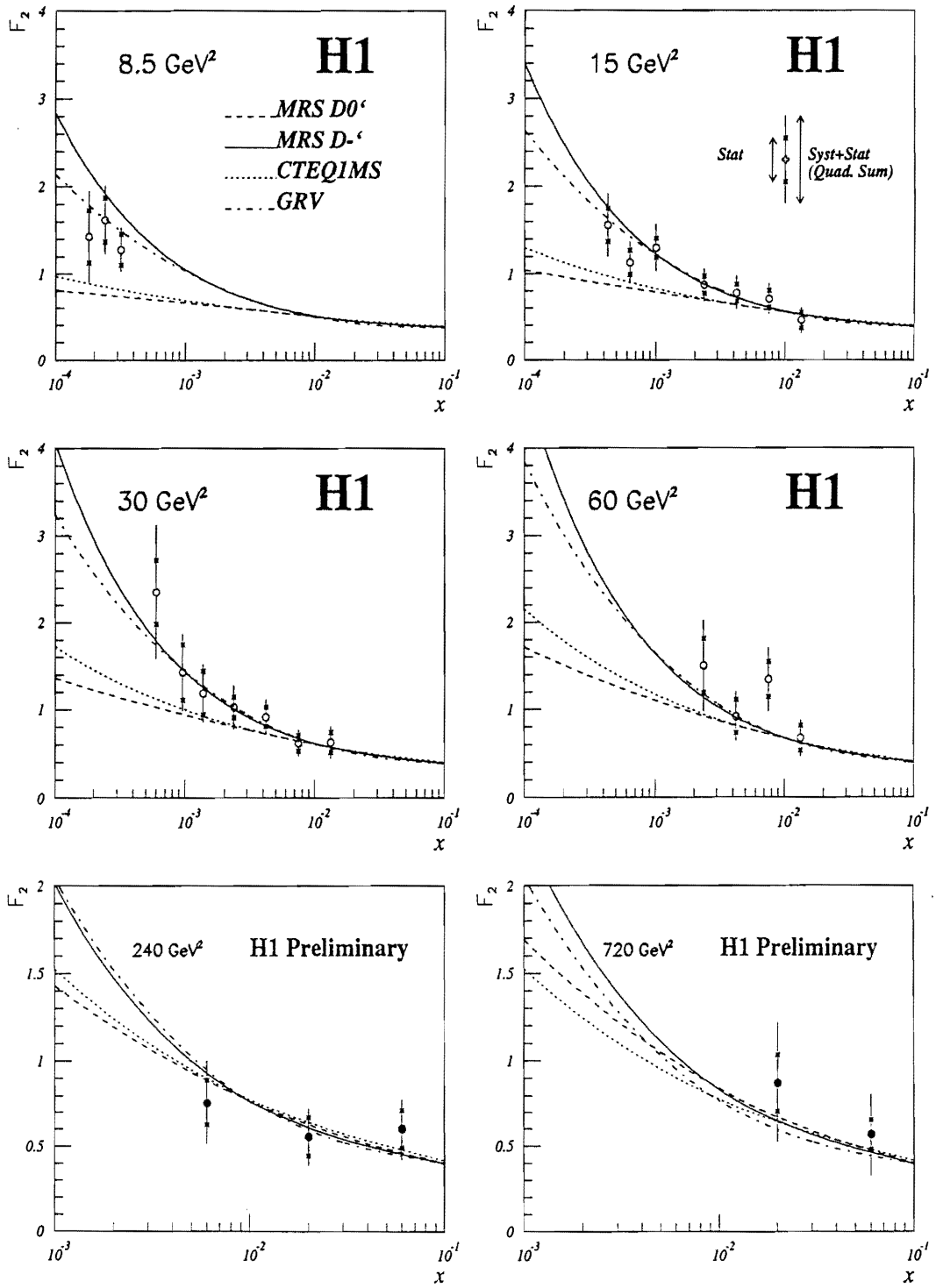

Figure 2: F_2^p *measurements of H1 compared with some parametrization predictions*

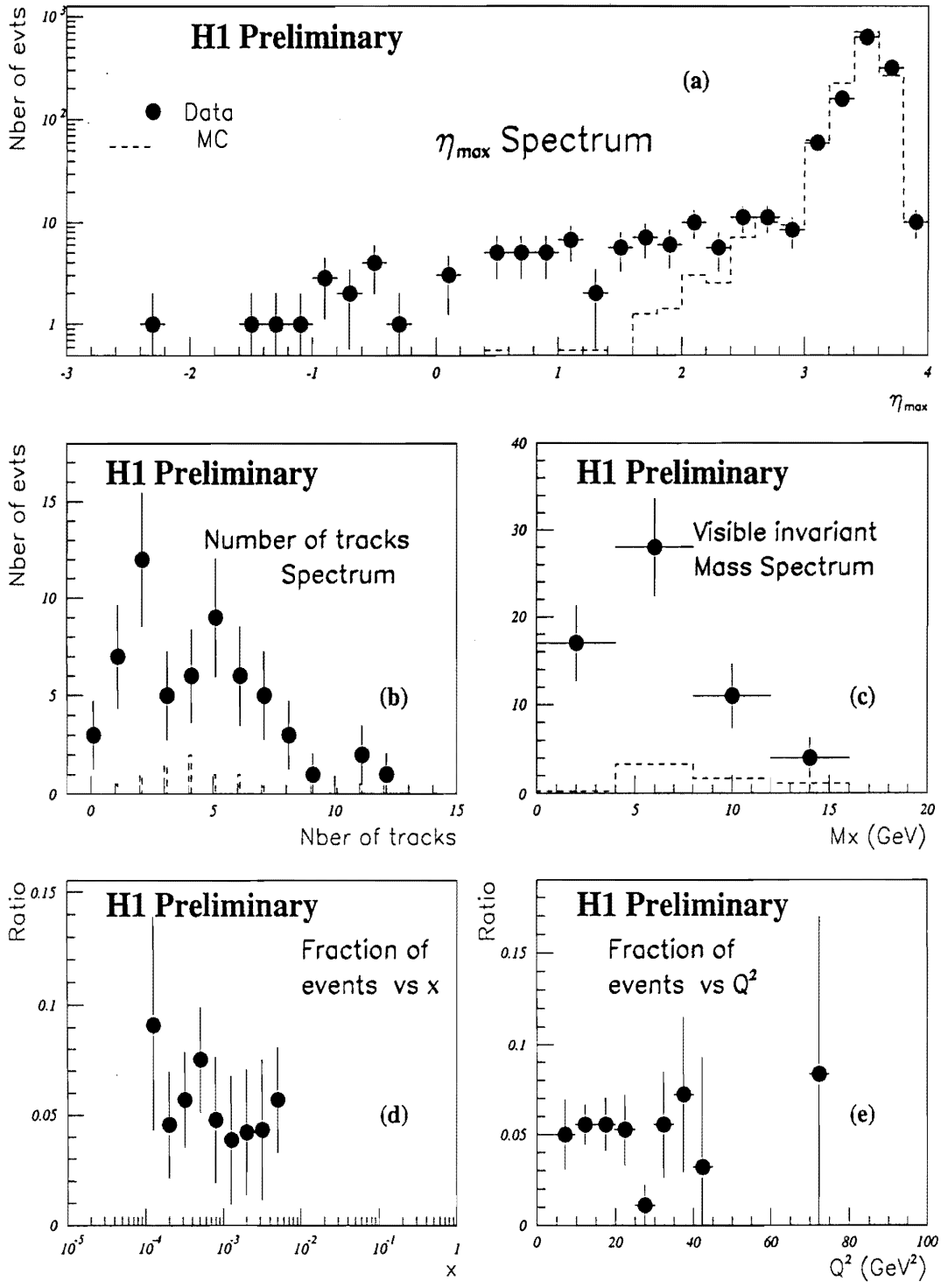

Figure 3: *Properties of large rapidity gap events*